Quantum binary particle swarm optimization for optimal on-load tap changing and power loss reduction

Aji Akbar Firdaus[1], Irrine Budi Sulistiawati[2], Vicky Andria Kusuma[3], Dimas Fajar Uman Putra[4], Hamzah Arof[5], Novian Patria Uman Putra[6], Sena Sukmananda Suprapto[3]
[1]Department of Engineering, Faculty of Vocational, Universitas Airlangga, Surabaya, Indonesia
[2]Department of Electrical Engineering, Faculty of Industrial Technology, Institut Teknologi Nasional Malang, Malang, Indonesia
[3]Department of Electrical Engineering, Faculty of Industrial and Process Technology, Institut Teknologi Kalimantan, Balikpapan, Indonesia
[4]Department of Electrical Engineering, Faculty of Intelligent Electrical and Informatics Technology, Institut Teknologi Sepuluh Nopember, Surabaya, Indonesia
[5]Department of Electrical Engineering, Faculty of Engineering, University of Malaya, Kuala Lumpur, Malaysia
[6]Department of Electrical Engineering, Faculty of Electrical Engineering and Information Technology, Institut Teknologi Adhi Tama, Surabaya, Indonesia

Article Info

Article history:

Received Sep 29, 2023
Revised Dec 22, 2023
Accepted Jan 12, 2024

Keywords:

On-load tap changers
Power loss
Quantum binary particle swarm optimization
Transformer
Voltage drop

ABSTRACT

Over time, there has been a continuous surge in the demand for electrical energy, necessitating the development of larger and more intricate electrical power networks. These extensive networks pose a significant challenge, primarily in the form of considerable loss of electrical energy, which, if not effectively addressed, may lead to persistent and imperceptible losses. In response to this challenge, this research proposes the application of quantum binary particle swarm optimization (QBPSO) for the coordinated management of on-load tap changers (OLTC) in loaded transformers within a distribution network, with a specific emphasis on reducing power losses. The experimental results demonstrate that the implementation of QBPSO results in a reduction of power loss from 21.756107 kW to 19.157321 kW and an increase in the average voltage from 19.00467941 kV to 19.93068 kV in a 20 kV 34-bus distribution network. This has the potential to significantly enhance overall system efficiency.

Corresponding Author:

Aji Akbar Firdaus
Department of Engineering, Faculty of Vocational, Universitas Airlangga
Surabaya, Jawa Timur, Indonesia
Email: aa.firdaus@vokasi.unair.ac.id

1. INTRODUCTION

With the passage of time, the demand for electrical energy continues to surge. This escalating need necessitates larger and more complex electrical power networks. However, as these extensive networks evolve, they bring forth a significant challenge. One such challenge is the substantial loss of electrical energy within the network, which, if left unaddressed, can lead to ongoing and imperceptible losses.

The growing demand for electricity due to population expansion has necessitated the installation of power systems with a larger capacity. However, as the capacity of a power system increases, so does its power loss and operational cost [1]-[3]. Numerous approaches have been proposed to reduce power loss, such as preventing voltage drop, reducing unbalanced phase loads, correcting power factors using capacitor banks, and optimizing the loading of power transformers [4]-[6]. Photovoltaics (PVs) have also been integrated into power systems to control voltage level fluctuations and reduce power loss [7]-[9]. Static compensator distribution [10] and voltage control on the transformer using on-load tap changers (OLTC) can also be used to achieve the same objective [11]. Distributed generators (DGs), wind turbines, and PVs can additionally support extra power demand and stabilize supplied voltages [12]-[16]. However, OLTC coordination and the exchange of reactive power from DGs, wind turbines, and PVs are time-consuming and expensive to install and maintain.

In this research, we propose the utilization of quantum binary particle swarm optimization (QBPSO) to facilitate OLTC coordination and minimize power losses within a distribution network. The choice of particle swarm optimization (PSO) as the optimization technique is rooted in its advantageous qualities, including speed and efficiency, ease of implementation, scalability, adaptiveness, and a balanced exploration-exploitation trade-off. This paper delves into issues related to power losses within distribution systems and elaborates on the proposed approach for OLTC coordination. Experimental results stemming from the implementation of the suggested method are presented, and a concise conclusion is provided.

2. METHOD

2.1. Transformer

The electromagnetic induction principle is utilized by an electrical device known as a transformer to transfer alternating voltage from one level to others [17]. The transformer comprises two types of coils, the primary and secondary coils, which are electrically separated but magnetically connected, as depicted in Figure 1. The working principle of a transformer is based on Ampere's law, which states that an electrical current can generate a magnetic field, and Faraday's law, which states that a magnetic field can generate an electric current [18], [19]. When the primary coil is connected to an alternating voltage supply, alternating flux is generated inside the laminated core. This flux induces self-induction in the primary coil and mutual induction in the secondary coil, resulting in magnetic flux in the secondary coil. If the load is connected to the secondary coil, the secondary current flows.

A simple transformer is composed of two insulated coils or wires and an iron core. The ratio of turns on a transformer can be determined using (1) and the number of turns on the transformer can impact the voltage and current produced on the secondary side. This concept is related to the calculation of the number of transformers turns using (2), where Np and Ns represent the number of primary and secondary turns, and Vp and Vs are the voltages on the primary and secondary sides, respectively. Lastly, Ip and Is indicate the currents on the primary and secondary sides.

$$n = \frac{N_s}{N_p} \tag{1}$$

$$\frac{N_s}{N_p} = \frac{V_p}{V_s} = \frac{I_s}{I_p} \tag{2}$$

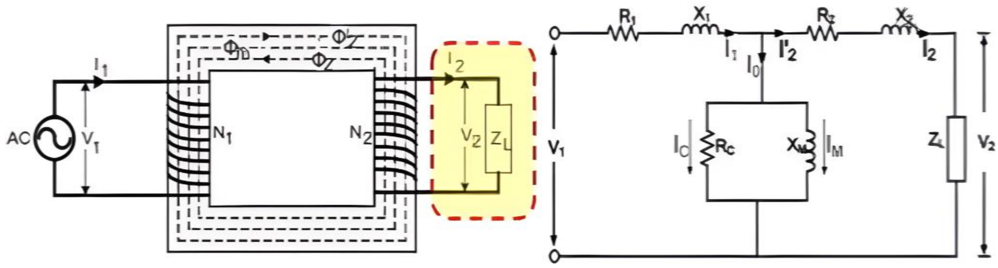

Figure 1. Transformer circuit

2.2. Problem formulation in the radial distribution network

The primary objective of this paper is to enhance the efficiency and economic viability of a distribution system by minimizing power loss while ensuring that the output voltage remains within specified limits. The overarching goal is to optimize the overall performance of the system by addressing both real and reactive power losses. Real power, which represents the actual energy consumed or dissipated as heat, and reactive power, associated with the phase difference between voltage and current in AC circuits, are targeted for reduction. In (3) and (4), as referenced from sources [20], [21], play a pivotal role in guiding the minimization process. By focusing on these equations, the paper aims to provide a systematic approach to achieving optimal power management, thereby contributing to the economic efficiency and sustainability of the distribution system.

$$Ploss = |BB(jj)^2|R(jj) \tag{3}$$

$$Qloss = |BB(jj)^2|X(jj) \tag{4}$$

2.3. Power flow in the distribution system

The power flow solution in a distribution system diverges from that in a transmission system due to the radial-connected network characteristic of distribution systems. A method commonly employed for power flow calculations in radial distribution systems is the bus injection to branch current–branch current to bus voltage (BIBC-BCBV) method, as outlined in references [22], [23]. This technique facilitates the accurate determination of power flow dynamics in the context of radial distribution networks. Figure 2 allows for the arrangement of the bus injection to bus current (BIBC) matrix, which can then be used to simplify (5) into (6).

$$[B_1\ B_2\ B_3\ B_4\ B_5\ ] = [1\ 1\ 1\ 1\ 1\ 0\ 1\ 1\ 1\ 1\ 0\ 0\ 1\ 1\ 0\ 0\ 0\ 0\ 1\ 0\ 0\ 0\ 0\ 0\ 1\ ][I_2\ I_3\ I_4\ I_5\ I_6\ ] \tag{5}$$

$$[B] = [BIBC][I] \tag{6}$$

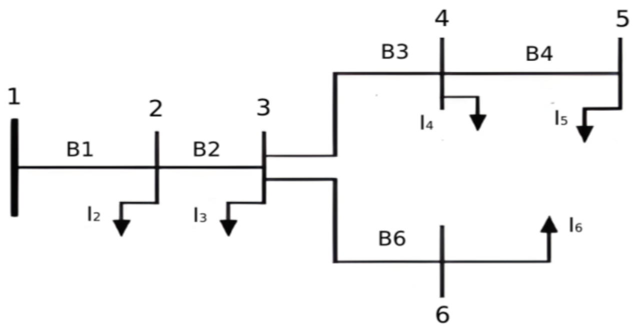

Figure 2. Single line diagram radial distribution network

The branch current to bus voltage (BCBV) matrix can be formulated from the voltage equation, as shown in (7).

$$\begin{aligned}&[V_1 - V_2\ V_1 - V_3\ V_1 - V_4\ V_1 - V_5\ V_1 - V_6\ ] =\\&[Z_{12}\ 0\ 0\ 0\ 0\ Z_{12}\ Z_{23}\ 0\ 0\ 0\ Z_{12}\ Z_{23}\ Z_{34}\ 0\ 0\ Z_{12}\ Z_{23}\ Z_{34}\ Z_{45}\ 0\ Z_{12}\ Z_{23}\ 0\ 0\ Z_{36}\ ]\\&[B_1\ B_2\ B_3\ B_4\ B_5\ ]\end{aligned} \tag{7}$$

Similarly, (7) can be simplified to (8).

$$[\Delta V]\ =\ [BCBV][B] \tag{8}$$

If (6) is substituted into (8), then ΔV can be expressed as (9) which in turn can be simplified to (10):

$$[\Delta V]=[BCBV][BIBC][I] \tag{9}$$

$$[\Delta V]=[DLF][I] \tag{10}$$

The complete power change can be obtained by iterating (5) through (13).

$$Ii(k)\ = \left(\frac{Pi+jQi}{Vi^{(k)}}\right)^* \tag{11}$$

$$[\Delta Vk]\ =\ [DLF][Ik] \tag{12}$$

$$[Vk+1]\ =\ [V1] - [\Delta Vk] \tag{13}$$

2.4. Quantum binary particle swarm optimization

The PSO algorithm, developed by Kennedy and Eberhart in 1995, draws inspiration from bird and fish colony intelligence [22]-[25]. In (14) and (15) are representative of the standard PSO algorithm. The introduction of the inertia weight as a diversity controller in the original PSO modifies the particle update equation.

$$v_i(t+1) = v_i(t) + c_1.rand(p_p - x_i(t)) + c_2.rand(p_g - x_i(t)) \tag{14}$$

$$x_i(t+1) = x_i(t) + v_i(t+1) \tag{15}$$

The standard procedure for implementing the PSO algorithm includes initializing the velocity, position, and PSO parameters, updating the velocity and position of the particles using (14) and (15), evaluating the fitness function with Pp and Pg update, comparing each candidate Pg from the fitness function value to get the best Pg value, and returning to step 2 if the value of Pg is not the best value. The iteration limit is performed to get Pg with the least or the best fitness function [26], [27]. The binary particle swarm optimization (BPSO) algorithm updates Pi and Pg in the swarm, with a difference in the interpretation of the velocity compared to the PSO standard. The range of the velocity in BPSO is limited to [0,1]. In (16) is used to obtain the new position of the particle, while its velocity is determined by (17).

$$v'_{ij}(t) = sig((t)) = \frac{1}{1+e^{-v_{ij}(t)}} \tag{16}$$

$$x_{ij}(t+1) = \begin{cases} 1 \; if \; r_{ij} < sig(v(t+1)) \\ \quad 0 \; otherwise \end{cases} \tag{17}$$

The integration between quantum computing and BPSO is known as QBPSO [28]-[30]. The use of the contraction-expansion coefficient is one of the parameter differentiators in QBPSO to control the convergence velocity from the particles. The first search, which is more global and dynamic, is accommodated by using an initial βmax value of 1. Then, the beta (β) value is gradually decreased until it reaches $\beta min = 0.4$. This is done to complete the QBPSO algorithm search with a better local search. In (18) gives the evolution of β.

$$\beta(t) = \beta_{max} - \left(\frac{\beta_{max}-\beta_{min}}{iter_{max}}\right).iter(t) \tag{18}$$

The new positions in quantum particle swarm optimization (QPSO) are provided by (19) and (20) respectively, using the Monte Carlo method. It is noteworthy that time units are used for particles to move. Additionally, in the migration process, there is an evaluation process, where the best position is represented by mbest. From the QPSO result, the velocity value will be converted to binary by using (16) and (17).

$$x_{id}(t+1) = p_{id}(t) + \beta(t).(mbest_d(t) - x_{id}(t)).ln\,ln\,(\tfrac{1}{u}), p_{id}(t) \geq 0.5 \tag{19}$$

$$x_{id}(t+1) = p_{id}(t) - \beta(t).(mbest_d(t) - x_{id}(t)).ln\,ln\,(\tfrac{1}{u}), p_{id}(t) < 0.5 \tag{20}$$

With $P_{id}(t)$ and $\varphi_d(t)$ values like (21) and (22).

$$p_{id}(t) = \varphi_d(t).pbest_{id}(t) + (1 - \varphi_d(t)).gbest_{id}(t) \tag{21}$$

$$\varphi_d(t) = \frac{c_1.r_{1d}(t)}{(c_1.r_{id}(t))+(c_2.r_{2d}(t))} \tag{22}$$

3. RESULTS AND DISCUSSION

In this research, a 20 kV 34-bus radial network is utilized with the OLTC's location on the IEEE 34 bus system depicted in Figure 3. The net and load data on each bus are presented in Tables 1 and 2. The bus data table includes a load-type column where the value 1 denotes constant power, 2 denotes constant current, and 3 represents constant impedance. In the system, there are 34 buses and five transformers, positioned between specific buses. The power flow in the radial distribution system is calculated using the BIBC-BCBV method with average lines and loads taken from (13). The total active power of the loads is 428.638399 kW. Without OLTC optimization, the power loss from the distribution system is 21.756107 kW, and the average voltage magnitude is 19.00467941 kV, with the lowest voltage at 18.5581 kV. These values are obtained with tap formation for transformers 1 to 5 in a sequence of -1, 0, 2, -1, 0.

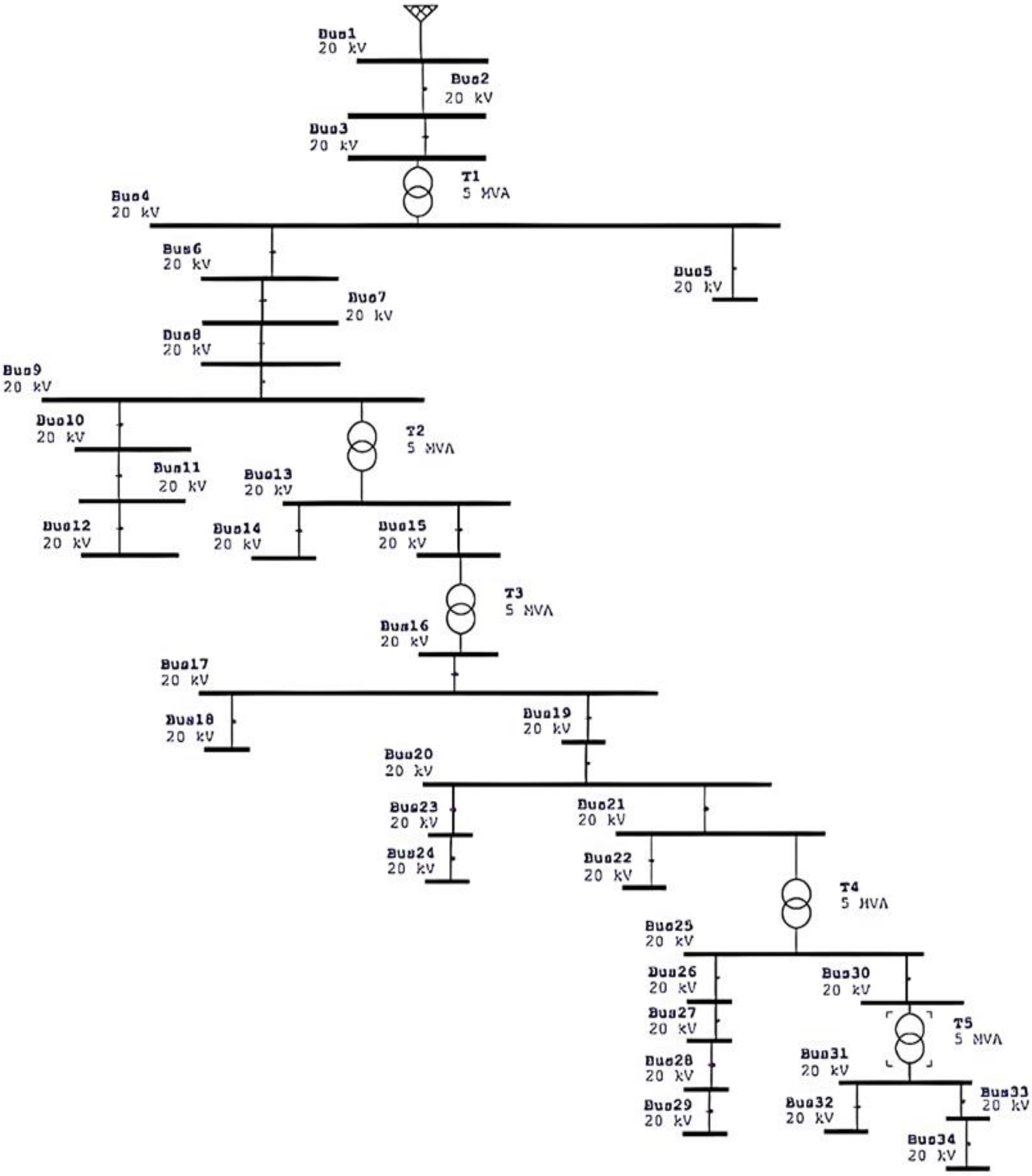

Figure 3. Single line diagram distribution system 34-bus

The voltage drops and current values in every bus and line obtained from the power flow simulation in Table 1 represent the condition or characteristic of the IEEE 34 bus system and are used to calculate the power loss. Figure 4 shows the bus voltage of the system within the defined tolerance range of ± 5% of the base voltage of 20 kV, where buses 16 to 34 experience under voltage. Tap formation for transformer 1 to transformer 5 is performed in a sequence of -1, 0, 2, -1, 0. The current at the line between bus 3 and 4 for transformer 1 is 20.7 A with tap transformer -1. Similarly, for transformer 2, the current at line 9 between bus 9 and 13 is 20.7 A with tap transformer 0. For transformer 3, the current at the line between bus 15 and bus 16 is 20.7 A with tap transformer 2. The current at the line between bus 21 and bus 25 for transformer 4 is 11.27 A with tap transformer -1, while for transformer 5, the obtained current is 0.57 A with tap transformer 0.

Table 1. Power flow result without OLTC optimization using QBPSO

From bus	To bus	Losses		Current		Voltage drops (kV)
		P (kW)	Q (kVAR)	I (A)	Angle (deg)	
1	2	0.26	0.26	20.07	-33.29	0.02
2	3	0.18	0.18	20.07	-33.29	0.01
3	4	3.29	3.28	20.07	-33.29	0.23
4	5	0	0	0	0	0
4	6	3.82	3.82	20.07	-33.29	0.26
6	7	3.03	3.03	20.07	-33.29	0.21
7	8	0	0	20.07	-33.29	0
8	9	0.05	0.03	20.07	-33.29	0
9	10	0	0	0	0	0
10	11	0	0	0	0	0
11	12	0	0	0	0	0
9	13	1.5	1.1	20.07	-33.29	0.09
13	14	0	0	0	0	0
13	15	0.65	0.34	20.07	-33.29	0.04
15	16	3.01	2.24	20.07	-33.29	0.19
16	17	0.07	0.05	19.55	-33.46	0
17	18	0	0	0	0	0
17	19	5.14	3.76	19.55	-33.46	0.33
19	20	0	0	19.55	-33.46	0
20	21	0.23	0.17	11.27	-38.58	0.02
21	22	0	0	0	0	0
20	23	0	0	8.39	-26.57	0
23	24	0.19	0.19	8.39	-26.57	0.03
21	25	0.27	0.2	11.27	-38.58	0.03
25	26	0.01	0.01	9.32	-38.54	0
26	27	0.04	0.03	9.32	-38.54	0.01
27	28	0	0	1.38	-39.2	0
28	29	0	0	1.38	-39.2	0
25	30	0	0	1.95	-38.82	0
30	31	0	0	0.57	-37.87	0
31	32	0	0	0.57	-37.87	0
31	33	0	0	0	0	0
33	34	0	0	0	0	0

Table 2. OLTC optimization result using QBPSO

	Line location		Tap transformer
	Initial bus	Final bus	
OLTC1	3	4	-1
OLTC2	9	13	1
OLTC3	15	16	3
OLTC4	21	25	-3
OLTC5	30	31	3

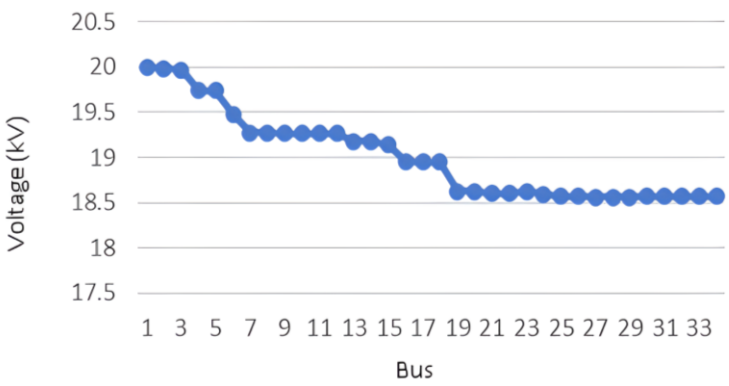

Figure 4. Voltage profile without OLTC optimization

The power loss simulation was performed to determine the active and reactive power losses in the transformer lines. The results showed that the active power losses in transformers 1, 2, and 3 were relatively high at 3.29 kW, 1.5 kW, and 3.01 kW, respectively, while the losses in transformers 4 and 5 were lower at

0.24 kW and 0 kW, respectively. The reactive power losses in all transformers were also recorded, with the highest value of 3.28 kVAR in transformer 1 and the lowest value of 0 kVAR in transformer 5. These losses were attributed to the large current flowing through the transformers. Furthermore, the voltage drop analysis revealed that the lines between bus 3 and bus 4, bus 15 and bus 16, and bus 21 and bus 25 had relatively high voltage drops of 0.23 kW, 0.19 kV, and 0.03 kV, respectively. The findings from this study provide valuable insights into the power loss and voltage drop characteristics of the IEEE 34 bus system, which could be useful for improving the system's overall efficiency and performance.

The QBPSO optimization simulation was utilized to obtain optimal OLTC tap coordination to minimize power loss and maintain voltage within a predetermined standard. The result of the OLTC simulation using QBPSO is presented in Table 2, which brings changes to the power flow in the system as shown in Table 3. The power loss obtained from this optimization is 19.157321 kW, with an average voltage of 19.93068 kV. Figure 5 indicates that there is no under-voltage bus, and the minimum voltage obtained is 19.099 kV. The required time for the optimization is 3.858783 seconds, as presented in Table 4.

Table 3. Power flow result with OLTC optimization using QBPSO

From bus	To bus	Losses		Current		Voltage drops (kV)
		P (kW)	Q (kVAR)	I (A)	Angle (deg)	
1	2	0.25	0.25	19.47	-33.53	0.02
2	3	0.17	0.17	19.47	-33.53	0.01
3	4	3.09	3.09	19.47	-33.53	0.22
4	5	0	0	0	0	0
4	6	3.6	3.59	19.47	-33.53	0.26
6	7	2.85	2.85	19.47	-33.53	0.2
7	8	0	0	19.47	-33.53	0
8	9	0.04	0.03	19.47	-33.53	0
9	10	0	0	0	0	0
10	11	0	0	0	0	0
11	12	0	0	0	0	0
9	13	1.14	0.77	19.47	-33.53	0.09
13	14	0	0	0	0	0
13	15	0.61	0.32	19.47	-33.53	0.04
15	16	2.36	1.55	19.47	-33.53	0.18
16	17	0.07	0.05	18.89	-33.73	0
17	18	0	0	0	0	0
17	19	4.8	3.52	18.89	-33.73	0.31
19	20	0	0	18.89	-33.73	0
20	21	0.23	0.17	11.37	-38.53	0.03
21	22	0	0	0	0	0
20	23	0	0	7.62	-26.57	0
23	24	0.16	0.16	7.62	-26.57	0.03
21	25	-0.26	-0.03	11.37	-38.53	0.03
25	26	0.01	0.01	9.51	-38.48	0
26	27	0.04	0.03	9.51	-38.48	0.01
27	28	0	0	1.34	-39.15	0
28	29	0	0	1.34	-39.15	0
25	30	0	0	1.86	-38.8	0
30	31	-0.02	-0.02	0.52	-37.87	0
31	32	0	0	0.52	-37.87	0
31	33	0	0	0	0	0
33	34	0	0	0	0	0

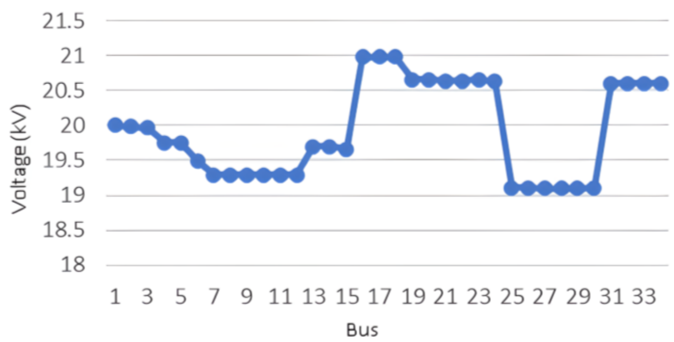

Figure 5. Voltage profile with OLTC optimization using QBPSO

Table 4. Comparison of time running program results

Method	Time
BPSO	10.5559
QDE	7.182868
QBPSO	3.858783

The tap formation for transformers 1 to 5 in sequence is used: -1, 1, 3, -3, 3. The current in the line between bus 3 and bus 4 is lowered from 20.7 A to 19.47 A with tap transformer -1 at transformer 1. The current in the line between bus 9 and bus 13 is lowered from 20.7 A to 19.47 A with tap transformer 1 at transformer 2. The current in the line between bus 15 and bus 16 is lowered from 20.7 A to 19.47 A with tap transformer 3 at transformer 3. The current in the line between bus 21 and 25 is increased from 11.27 A to 11.37 A with tap transformer -3 at transformer 4. The current from 0.57 A to 0.52 A is obtained with tap transformer 3 at transformer 35. From the obtained current with the tap transformer, it can be seen that the current flowing can be reduced, resulting in a decrease in power losses.

The simulated power loss in the lines with transformers shows that the active power loss in the line of the transformer 1 decreased from 3.29 kW to 3.09 kW and the reactive power loss decreased from 3.28 kVAR to 3.09 kVAR. The active power loss in the line of transformer 2 decreased from 1.5 kW to 1.14 kW and the reactive power loss decreased from 1.1 kVAR to 0.07 kVAR. The active power loss in the line of transformer 3 decreased from 3.01 kW to 2.36 kW and the reactive power loss decreased from 2.24 kVAR to 1.55 kVAR. The active power loss in the line of the transformer 4 decreased from 0.27 kW to -0.26 kW and the reactive power loss decreased from 0.2 kVAR to 0.03 kVAR. The active power loss in the line of transformer 5 decreased from 0 kW to -0.02 kW and the reactive power loss decreased from 0 kVAR to -0.02 kVAR. The voltage drops across the lines between bus 3 and bus 4 decreased from 0.23 kV to 0.22 kV, the voltage drops in the line between bus 9 and bus 13 remained at 0.09 kV, the voltage drops in the line between bus 15 and bus 16 decreased from 0.19 kV to 0.18 kV, the voltage drops in the line between bus 21 and bus 25 remained at 0.03 kV, and the voltage drop in the line between bus 30 and bus 31 remained at 0.0 kV. Table 5 presents a comparison of simulation results using various artificial intelligence methods. In this paper, GA, BPSO, QDE, and QBPSO are compared to QBPSO. Based on Table 5, it is shown that QBPSO converges faster than the other methods, as demonstrated in Table 4. In the first experiment, QBPSO was able to directly find the minimum power loss of 19.1573 kW, while GA produced a simulation result of 19.3016 kW.

Table 5. Comparison of running program results

No	GA	BPSO	QDE	QBPSO
1	19.8232	19.3411	19.3718	19.1573
2	19.8232	19.3718	19.1573	19.6779
3	19.8232	19.1573	19.1573	19.4044
4	19.7020	19.1878	19.1878	19.3718
5	19.7020	19.2201	19.1573	19.7060
6	19.3016	19.6484	19.3411	19.4389
7	19.5169	19.2201	19.1573	19.4044
8	19.6834	19.1573	19.3411	19.2545
9	19.7602	19.2201	19.3411	19.4389
10	19.6828	19.3411	19.1573	19.4279
Mean	19.6819	19.2865	19.2370	19.4282
STD	0.162869	0.149271	0.097111	0.165871
Worst	19.8232	19.6484	19.3718	19.7060
Best	19.3016	19.1573	19.1573	19.1573

4. CONCLUSION

The QBPSO method was employed in this paper to determine the optimal arrangement of tap transformers in a network for the purpose of minimizing power loss and improving the average voltage level. The tested IEEE 34 bus system was found to have a power loss of 21.756107 kW and an average voltage magnitude of 19.00467941 kV, with the lowest voltage recorded at 18.5581 kV. The OLTC values for transformers 1 to 5 in sequence were -1, 0, 2, -1, and 0. Through OLTC optimization, QBPSO simulation resulted in a power loss of 19.157321 kW and an average voltage of 19.93068 kV, with OLTC values for transformers 1 to 5 in the sequence being -1, 1, 3, -3, and 3.

REFERENCES

[1] U. Agarwal and N. Jain, “Distributed Energy Resources and Supportive Methodologies for their Optimal Planning under Modern Distribution Network: a Review,” *Technology and Economics of Smart Grids and Sustainable Energy*, vol. 4, no. 1, pp. 1-21, Jan. 2019, doi: 10.1007/s40866-019-0060-6.

[2] H. S. Bidgoli and T. V. Cutsem, “Combined Local and Centralized Voltage Control in Active Distribution Networks,” *IEEE Transactions on Power Systems*, vol. 33, no. 2, pp. 1374–1384, Mar. 2018, doi: 10.1109/tpwrs.2017.2716407.

[3] Suyanto, Soedibyo, and A. A. Firdaus, “Design and simulation of Neural Network Predictive Controller pitch-angle in permanent magnetic synchronous generator wind turbine variable pitch system,” *2014 The 1st International Conference on Information Technology, Computer, and Electrical Engineering*, Nov. 2014, pp. 346-350, doi: 10.1109/icitacee.2014.7065769.

[4] S. Ding, Z. Zhang, Y. Sun, and S. Shi, “Multiple birth support vector machine based on dynamic quantum particle swarm optimization algorithm,” *Neurocomputing*, vol. 480, pp. 146–156, Apr. 2022, doi: 10.1016/j.neucom.2022.01.012.

[5] T. Zhou, Q. Long, K. M. Y. Law, and C. Wu, “Multi-objective stochastic project scheduling with alternative execution methods: An improved quantum-behaved particle swarm optimization approach,” *Expert Systems with Applications*, vol. 203, p. 117029, Oct. 2022, doi: 10.1016/j.eswa.2022.117029.

[6] N. Priyadarshi, S. Padmanaban, J. B. Holm-Nielsen, F. Blaabjerg, and M. S. Bhaskar, "An Experimental Estimation of Hybrid ANFIS–PSO-Based MPPT for PV Grid Integration Under Fluctuating Sun Irradiance," in *IEEE Systems Journal*, vol. 14, no. 1, pp. 1218-1229, Mar. 2020, doi: 10.1109/JSYST.2019.2949083.

[7] O. Llerena-Pizarro, N. Proenza-Perez, C. E. Tuna, and J. L. Silveira, "A PSO-BPSO Technique for Hybrid Power Generation System Sizing," in *IEEE Latin America Transactions*, vol. 18, no. 8, pp. 1362-1370, Aug. 2020, doi: 10.1109/TLA.2020.9111671.

[8] V. Veerasamy *et al*., "A Hankel Matrix Based Reduced Order Model for Stability Analysis of Hybrid Power System Using PSO-GSA Optimized Cascade PI-PD Controller for Automatic Load Frequency Control," in *IEEE Access*, vol. 8, pp. 71422-71446, 2020, doi: 10.1109/ACCESS.2020.2987387.

[9] R. Małkowski, M. Izdebski, and P. Miller, “Adaptive Algorithm of a Tap-Changer Controller of the Power Transformer Supplying the Radial Network Reducing the Risk of Voltage Collapse,” *Energies*, vol. 13, no. 20, p. 5403, Oct. 2020, doi: 10.3390/en13205403.

[10] L. A. Kumar and S. A. Alexander, “A Voltage-Controlled DSTATCOM for Power Quality Improvement,” *Computational Paradigm Techniques for Enhancing Electric Power Quality*, pp. 163–171, Nov. 2018, doi: 10.1201/9780429442711-3.

[11] A. N. Hasan and N. Tshivhase, “Voltage regulation system for OLTC in distribution power systems with high penetration level of embedded generation,” *International Transactions on Electrical Energy Systems*, vol. 29, no. 7, p. e12111, Jun. 2019, doi: 10.1002/2050-7038.12111.

[12] M. Bazrafshan, N. Gatsis, and H. Zhu, “Optimal Power Flow with Step-Voltage Regulators in Multi-Phase Distribution Networks,” *IEEE Transactions on Power Systems*, vol. 34, no. 6, pp. 4228–4239, Nov. 2019, doi: 10.1109/tpwrs.2019.2915795.

[13] S.-B. Kim and S.-H. Song, “A Hybrid Reactive Power Control Method of Distributed Generation to Mitigate Voltage Rise in Low-Voltage Grid,” *Energies*, vol. 13, no. 8, p. 2078, Apr. 2020, doi: 10.3390/en13082078.

[14] N. Tshivhase, A. N. Hasan, and T. Shongwe, “Proposed Fuzzy Logic System for Voltage Regulation and Power Factor Improvement in Power Systems with High Infiltration of Distributed Generation,” *Energies*, vol. 13, no. 16, p. 4241, Aug. 2020, doi: 10.3390/en13164241.

[15] M. Chamana and B. H. Chowdhury, “Optimal Voltage Regulation of Distribution Networks with Cascaded Voltage Regulators in the Presence of High PV Penetration,” *IEEE Transactions on Sustainable Energy*, vol. 9, no. 3, pp. 1427–1436, Jul. 2018, doi: 10.1109/tste.2017.2788869.

[16] A. A. Firdaus, R. T. Yunardi, E. I. Agustin, T. E. Putri, and D. O. Anggriawan, “Short-term photovoltaics power forecasting using Jordan recurrent neural network in Surabaya,” *TELKOMNIKA (Telecommunication Computing Electronics and Control)*, vol. 18, no. 2, pp. 1089-1094, Apr. 2020, doi: 10.12928/telkomnika.v18i2.14816.

[17] F. Bai, R. Yan, T. Saha, and D. Eghbal, “A New Remote Tap Position Estimation Approach for Open-Delta Step-Voltage Regulator in a Photovoltaic Integrated Distribution Network,” *2019 IEEE Power & Energy Society General Meeting (PESGM)*, vol. 33, no. 4, pp. 4433-4443, Jul. 2018, doi: 10.1109/TPWRS.2017.2776311.

[18] A. Del Pizzc, L. Di Noia, D. Lauria, M. Crispino, A. Cantiello, and F. Mottola, “Control of OLTC distribution transformer addressing voltage regulation and lifetime preservation,” *2018 International Symposium on Power Electronics, Electrical Drives, Automation and Motion (SPEEDAM)*, Amalfi, Italy, 2018, pp. 1002-1007, doi: 10.1109/SPEEDAM.2018.8445294.

[19] N. Tshivhase, A. N. Hasan, and T. Shongwe, “A Fault Level-Based System to Control Voltage and Enhance Power Factor Through an On-Load Tap Changer and Distributed Generators,” *IEEE Access*, vol. 9, pp. 34023–34039, 2021, doi: 10.1109/access.2021.3061622.

[20] M. Aryanezhad, “Management and coordination of LTC, SVR, shunt capacitor and energy storage with high PV penetration in power distribution system for voltage regulation and power loss minimization,” *International Journal of Electrical Power & Energy Systems*, vol. 100, pp. 178–192, Sep. 2018, doi: 10.1016/j.ijepes.2018.02.015.

[21] K. Kotsalos, I. Miranda, J. L. Dominguez-Garcia, H. Leite, N. Silva, and N. Hatziargyriou, “Exploiting OLTC and BESS Operation Coordinated with Active Network Management in LV Networks,” *Sustainability*, vol. 12, no. 8, p. 3332, Apr. 2020, doi: 10.3390/su12083332.

[22] M. Ali *et al*., “The comparison of dual axis photovoltaic tracking system using artificial intelligence techniques,” *IAES International Journal of Artificial Intelligence (IJ-AI)*, vol. 10, no. 4, pp. 901-909, Dec. 2021, doi: 10.11591/ijai.v10.i4.pp901-909.

[23] A. A. Firdaus, R. T. Yunardi, E. I. Agustin, S. D. N. Nahdliyah, and T. A. Nugroho, “An improved control for MPPT based on FL-PSo to minimize oscillation in photovoltaic system,” *International Journal of Power Electronics and Drive Systems (IJPEDS)*, vol. 11, no. 2, pp. 1082-1087, Jun. 2020, doi: 10.11591/ijpeds.v11.i2.pp1082-1087.

[24] A. A. Firdaus, O. Penangsang, A. Soeprijanto, and D. F. U.P., “Distribution Network Reconfiguration Using Binary Particle Swarm Optimization to Minimize Losses and Decrease Voltage Stability Index,” *Bulletin of Electrical Engineering and Informatics*, vol. 7, no. 4, pp. 514–521, Dec. 2018, doi: 10.11591/eei.v7i4.821.

[25] Q. Wu, Y. Shen, Z. Ma, J. Fan, and R. Ge, “iBQPSO: an Improved BQPSO Algorithm for Feature Selection,” *2018 International Joint Conference on Neural Networks (IJCNN),* Rio de Janeiro, Brazil, 2018, pp. 1-8, doi: 10.1109/IJCNN.2018.8489676/

[26] S. K. Sahoo, E. H. Houssein, M. Premkumar, A. K. Saha, and M. M. Emam, “Self-adaptive moth flame optimizer combined with crossover operator and Fibonacci search strategy for COVID-19 CT image segmentation,” *Expert Systems with Applications*, vol. 227, p. 120367, Oct. 2023, doi: 10.1016/j.eswa.2023.120367.

[27] S. Chakraborty, A. K. Saha, and A. Chhabra, "Improving Whale Optimization Algorithm with Elite Strategy and Its Application to Engineering-Design and Cloud Task Scheduling Problems," *Cognitive Computation*, vol. 15, no. 5, pp. 1497–1525, Jan. 2023, doi: 10.1007/s12559-022-10099-z.
[28] S. Sharma, A. K. Saha, S. Roy, S. Mirjalili, and S. Nama, "A mixed sine cosine butterfly optimization algorithm for global optimization and its application," *Cluster Computing*, vol. 25, no. 6, pp. 4573–4600, 2022, doi: 10.1007/s10586-022-03649-5.
[29] S. Chakraborty, A. K. Saha, S. Sharma, S. K. Sahoo, and G. Pal, "Comparative Performance Analysis of Differential Evolution Variants on Engineering Design Problems," *Journal of Bionic Engineering*, vol. 19, no. 4, pp. 1140–1160, Jun. 2022, doi: 10.1007/s42235-022-00190-4.
[30] S. Sharma, A. K. Saha, A. Majumder, and S. Nama, "MPBOA-A novel hybrid butterfly optimization algorithm with symbiosis organisms search for global optimization and image segmentation," *Multimedia Tools and Applications*, vol. 80, no. 8, pp. 12035–12076, Jan. 2021, doi: 10.1007/s11042-020-10053-x.

BIOGRAPHIES OF AUTHORS

Aji Akbar Firdaus received a Master of Engineering in the Department of Electrical Engineering, Institut Teknologi Sepuluh Nopember (ITS), Surabaya, Indonesia, in 2015. He is currently a lecturer and researcher in the Department of Engineering, Universitas Airlangga. His research interests include power systems simulation, power systems analysis, power systems stability, renewable energy, and artificial intelligence. He can be contacted at email: aa.firdaus@vokasi.unair.ac.id.

Irrine Budi Sulistiawati received a doctor degree from the Department of Electrical Engineering, Institut Teknologi Sepuluh Nopember. She is currently a lecturer and researcher at Electrical Engineering Institut Teknologi Nasional Malang Indonesia since 2003. Her research interests in transient stability, power system stability, renewable energy, and artificial intelligence. She can be contacted at email: irrine@lecturer.itn.ac.id.

Vicky Andria Kusuma was born in Indonesia. He received an engineering degree in Electrical Engineering from the Politeknik Elektronika Negeri Surabaya, Indonesia, and a master's degree in Electrical Engineering from the Institut Teknologi Sepuluh Nopember in Indonesia. He is currently a lecturer in Electrical Engineering at the Kalimantan Institute of Technology in Indonesia. He can be contacted at email: vickyandria@lecturer.itk.ac.id.

Dimas Fajar Uman Putra was born in Surabaya on November 8, 1988. He completed his undergraduate program at the Electrical Engineering Department, ITS Surabaya in 2010 and then continued his master's program at the Electrical Engineering department, ITS Surabaya and completed it in 2012. Finally, he received his Dr. Eng. from the Electrical Engineering Fepartment, Institut Teknologi Sepuluh Nopember in 2018. He is currently a lecturer and researcher at Institut Teknologi Sepuluh Nopember. His research interests include voltage stability, renewable energy, and power system. He can be contacted at email: dimasfup@ee.its.ac.id.

Hamzah Arof is a professor of electrical engineering at the University of Malaya, Malaysia. He is interested in signal processing, photonics, and econometrics. He can be contacted at email: ahamzah@um.edu.my.

Novian Patria Uman Putra is a lecturer and researcher at the Department of Electrical Engineering, Institut Teknologi Adhi Tama Surabaya, Surabaya, Indonesia. He is interested in voltage stability and power system. He can be contacted at email: novian111190@itats.ac.id.

Sena Sukmananda Suprapto received his bachelor degree in Engineering Physics at Institut Teknologi Sepuluh Nopember and his master degree in Electrical Engineering at Institut Teknologi Bandung. He is a lecturer at bachelor degree in Electrical Engineering at Institut Teknologi Kalimantan. His research lines are computer vision, biomechanics, sports science, and IoT. He can be contacted at email: s.s.suprapto@lecturer.itk.ac.id.